

3-23-2026

Colorimetric Detection of Mercury (II) Ions Utilizing Bio-Colloidal Silver Nanoparticles Synthesized Via Microwave-Assisted Method with Matoa Leaf Extract

Ari Sulisty Rini

Department of Physics, Faculty of Mathematics and Natural Sciences, Universitas Riau, Pekanbaru 28293, Indonesia, ari.sulistyo@lecturer.unri.ac.id

Yolanda Rati

Department of Physics, Faculty of Sciences, Institut Teknologi Sumatera, Lampung Selatan 35365, Indonesia, yolanda.rati@fi.itera.ac.id

Gilar Adnan Ramadhan

Department of Physics, Faculty of Mathematics and Natural Sciences, Universitas Riau, Pekanbaru 28293, Indonesia, gilar.adnan0303@student.unri.ac.id

Yan Soerbakti

Department of Physics, Faculty of Mathematics and Natural Sciences, Universitas Riau, Pekanbaru 28293, Indonesia, yansoerbakti2@gmail.com

Lazuardi Umar

Department of Physics, Faculty of Mathematics and Natural Sciences, Universitas Riau, Pekanbaru 28293, Indonesia, lazuardi@lecturer.unri.ac.id

Follow this and additional works at: <https://bsj.uobaghdad.edu.iq/home>

How to Cite this Article

Rini, Ari Sulisty; Rati, Yolanda; Ramadhan, Gilar Adnan; Soerbakti, Yan; and Umar, Lazuardi (2026) "Colorimetric Detection of Mercury (II) Ions Utilizing Bio-Colloidal Silver Nanoparticles Synthesized Via Microwave-Assisted Method with Matoa Leaf Extract," *Baghdad Science Journal*: Vol. 23: Iss. 3, Article 18. DOI: <https://doi.org/10.21123/2411-7986.5236>

This Article is brought to you for free and open access by Baghdad Science Journal. It has been accepted for inclusion in Baghdad Science Journal by an authorized editor of Baghdad Science Journal. For more information, please contact mina.t@csj.uobaghdad.edu.iq.



RESEARCH ARTICLE

Colorimetric Detection of Mercury (II) Ions Utilizing Bio-Colloidal Silver Nanoparticles Synthesized Via Microwave-Assisted Method with Matoa Leaf Extract

Ari Sulisty Rini^{1,*}, Yolanda Rati², Gilar Adnan Ramadhan¹, Yan Soerbakti¹, Lazuardi Umar¹

¹ Department of Physics, Faculty of Mathematics and Natural Sciences, Universitas Riau, Pekanbaru 28293, Indonesia

² Department of Physics, Faculty of Sciences, Institut Teknologi Sumatera, Lampung Selatan 35365, Indonesia

ABSTRACT

In this work, bio-colloidal silver nanoparticles (AgNPs) were synthesized using Matoa (*Pometia pinnata*) leaf extract as a reducing and stabilizing agent under microwave irradiation to promote rapid AgNPs formation. The influence of microwave irradiation powers (360, 540, and 720 W) on the optical, structural, and morphological properties of the synthesized AgNPs was systematically investigated. The AgNPs formation was characterized by yellowish-brown colloids formation with surface plasmon resonant (SPR) bands centered around 430 nm, as detected by UV-Vis spectroscopy. FTIR analysis revealed the presence of C-H and O-H functional groups from polyphenols and flavonoids in Ag⁺ ion reduction. XRD pattern revealed a face-centered cubic (FCC) crystalline structure of AgNPs, while TEM images showed predominantly quasi-spherical morphology with average diameter of 58–62 nm. The colorimetric sensing performance was examined over Hg²⁺ concentration ranging from 1–100 ppm. Upon Hg²⁺ exposure, the AgNPs colloids demonstrated a progressive decrease in SPR intensity along with visible discoloration in the 350–550 nm region. Nanoparticles synthesized at 720 W exhibited the highest sensitivity of AgNPs, which displayed obvious discoloration observed in the range 40–100 ppm of Hg²⁺ with steepest slope at 8×10^{-4} . These findings highlight the potential of microwave-assisted *Pometia pinnata*-derived AgNPs as a green and eco-friendly approach for the colorimetric sensing of mercury ions.

Keywords: Bio-colloidal, Mercury (II) ions, Microwave-assisted synthesis, *Pometia pinnata* leaf, Silver nanoparticles

Introduction

The demand for clean water continues to increase alongside population growth and industrial development. In Indonesia, particularly in Riau Province, mercury contamination has become a serious environmental concern due to illegal gold mining activities along the Kuantan River watershed.¹ Mercury is a toxic substance that can cause damage to the brain, nervous system, and kidneys.² The monitoring and detection of mercury levels has recently

become a subject of considerable interest. The detection of mercury using atomic absorption spectrometry, voltammetry, and inductively coupled plasma atomic emission spectrometry has been widely reported.^{3–5} Several limitations including complicated procedures and time-consuming and expensive equipment, make these methods less effective.⁶

Colorimetric sensors using silver nanoparticles (AgNPs) are considered to be among the most promising alternatives, given their ability to provide high surface energy and enhance surface reactivity

Received 30 May 2025; revised 5 October 2025; accepted 19 October 2025.
Available online 23 March 2026

* Corresponding author.

E-mail addresses: ari.sulisty@lecturer.unri.ac.id (A. S. Rini), yolanda.rati@fi.itera.ac.id (Y. Rati), gilar.adnan0303@student.unri.ac.id (G. A. Ramadhan), yansoerbakti2@gmail.com (Y. Soerbakti), lazuardi@lecturer.unri.ac.id (L. Umar).

<https://doi.org/10.21123/2411-7986.5236>

2411-7986/© 2026 The Author(s). Published by College of Science for Women, University of Baghdad. This is an open-access article distributed under the terms of the Creative Commons Attribution 4.0 International License, which permits unrestricted use, distribution, and reproduction in any medium, provided the original work is properly cited.

through the mechanism of adsorption and catalysis.⁷ The properties of AgNPs possess electrical, optical, and mechanical properties with various applications, including catalysis, biosensing, bio-nanotechnology, imaging, and antimicrobial activity.⁸ AgNPs are most commonly found in the form of nanotubes, nanorods, nanocapsules, and nanoemulsions.⁹ They have surface plasmonic absorption bands that are observable with the naked eye, thus rendering them effective readout sensors and treatment of pollutants in water.^{10,11} Furthermore, the development of AgNPs in view of their SPR has the potential to provide effective, affordable, and accessible therapies for the majority of patients exposed to heavy metals via colorimetric methods.¹² Therefore, the colorimetric approach offers a practical alternative for detecting mercury (II) ions.

AgNPs can be prepared through physical, chemical, and biological methods. Physical and chemical approaches often require high-energy consumption, high-cost equipment, and the use of toxic reagents such as NaBH_4 or citrate. These chemicals may raise secondary environmental and safety concerns.¹³ In addition, structural defects are frequently identified in AgNPs produced by these methods.¹⁴ The biological approach (green synthesis) is preferred as it employs simple, environmentally friendly, and biocompatible materials. The synthesis of nanoparticles by this method involves the use of compounds found in microorganisms, plants, and viruses. Secondary metabolites in plant extracts, such as phenolics, alkaloids, and flavonoids, may act as both reducing and stabilizing agents during nanoparticle formation.¹⁵ Plant extracts are widely used due to the simplicity, affordability, and safety of the extraction procedure. The synthesis of AgNPs has been reported employing various plant extracts, such as *Terminalia catappa*, *Actinidia deliciosa*, *Buddleja globosa*, and *Matricaria recutita*.^{16–19} Matoa leaves contain significant quantities of flavonoids, phenolics, tannins, and saponins. These phytochemicals facilitate Ag^+ reduction and contribute to Ag^0 colloidal stabilizers.²⁰ Previous studies have reported Matoa leaf extract as an effective reducing agent in the green synthesis of ZnO nanoparticles, where the secondary metabolites regulated the particle morphology and enhanced the photocatalytic activity. The high polyphenol content and local availability of Matoa leaves support their suitability as a reducing agent for AgNPs synthesis.

This study employed matoa leaf extract for the microwave-assisted synthesis of bio-colloidal AgNPs. The microwave heating was used due to its rapid heating, low energy consumption, and ability to produce a uniform nanoparticle distribution. The use

of microwave technique has also demonstrated to enhance the extraction of polyphenolic compounds compared to conventional methods.²¹ Preliminary studies shown that increasing microwave power leads to accelerated nucleation, resulting in smaller and more uniform nanoparticles. Based on these findings, irradiation powers of 360, 540, and 720 W were applied to synthesize AgNPs. The obtained AgNPs were characterized using UV-Vis spectroscopy, Fourier-transform infrared spectroscopy (FTIR), X-ray diffraction (XRD), and transmission electron microscopy (TEM). The sensitivity of AgNPs for detecting Hg(II) ions was assessed using HgCl_2 solution with concentrations ranging from 1 to 100 ppm.

Materials and methods

Materials

Fresh Matoa (*Pometia pinnata*) leaves were collected from the Riau University campus area. The collected leaves were rinsed thoroughly with distilled water to remove surface impurities, air-dried at room temperature, and subsequently oven-dried until constant weight was achieved. Silver nitrate (AgNO_3 , EMSURE®) and mercury (II) chloride (HgCl_2 , Smart Lab) were used without further purification. Distilled water was utilized as a solvent throughout the experiment.

Synthesis of bio-colloidal AgNPs

The extraction of Matoa leaf was involved the amalgamation of 2 g of powdered matoa leaves with 100 mL of distilled water within a conical flask. The mixture was subjected to heating at a temperature of 100°C for a duration of 10 minutes. Subsequently, the mixture was filtered through Whatman No. 1 filter paper to yield an aqueous extract. Subsequently, an aqueous solution of 3 mM silver nitrate was added to the extract, and the resulting mixture was irradiated in a microwave oven at three different power levels (360, 540, and 720 W) for 90 seconds. The schematic representation of the synthesis process is shown in Fig. 1.

Characterization techniques

The formation of silver nanoparticles (AgNPs) was monitored using a UV-Vis spectrophotometer (Agilent Cary 60) in the wavelength range of 300–600 nm. The functional groups present in the leaf extract and synthesized AgNPs were analyzed using a Fourier-transform infrared (FT-IR)

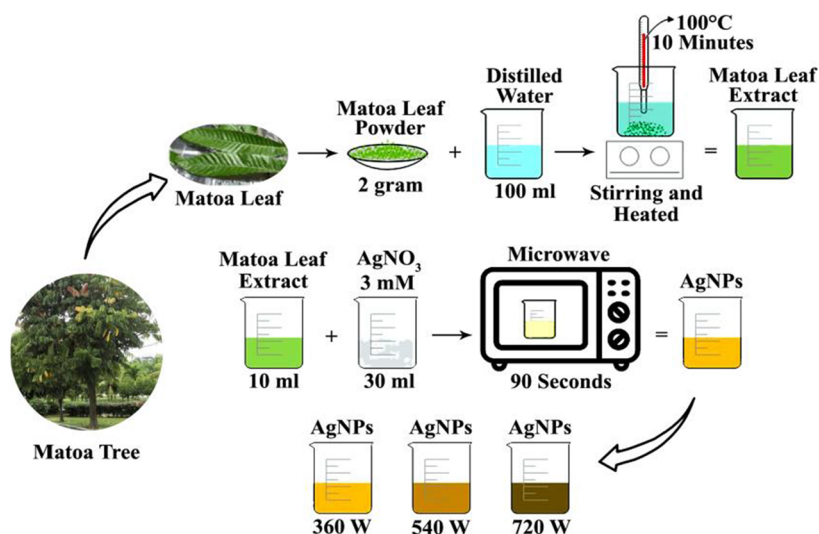


Fig. 1. Schematic of bio-colloidal AgNPs synthesis by microwave irradiation.

spectrophotometer (SHIMADZU IR Prestige-21) in the range of 4000–500 cm^{-1} . The crystalline structure was determined by X-ray diffraction (XRD) using an X'pert Pro PANalytical diffractometer with Cu K α radiation ($\lambda_{\text{CuK}\alpha} = 1.541 \text{ \AA}$). The surface morphology and particle size were investigated using transmission electron microscopy (Tecnai-20F Lorentz TEM).

Procedure for colorimetric sensor

The colorimetric detection of mercury (II) ions (Hg^{2+}) was evaluated through the mixing of 1 mL of bio-colloidal AgNPs with 2 mL of HgCl_2 solution at varying concentrations: 1, 5, 10, 15, 20, 40, 60, 80, and 100 ppm (1 ppm \approx 4.99 μM). The sensitivity of AgNPs was evaluated through visual observation of colloid discoloration and confirmed by SPR peak reduction using a UV-Vis spectrophotometer. The colorimetric sensitivity of AgNPs was evaluated from the linear curve slope of absorbance versus Hg (II) concentration.

Results and discussion

UV-Vis analysis

The formation of AgNPs was indicated by a visible color transition in the synthesis solution, as shown in Fig. 2a. Prior to the irradiation process, the mixture of silver nitrate (AgNO_3) and matoa leaf extract exhibited a pale-yellow coloration. After microwave irradiation, it was evident that the solution progressively darkened as the applied microwave power increased. AgNPs synthesized at 360, 540, and 720 W displayed dark yellow, reddish-brown, and

deep brown colors, respectively. This transformation reflects the reduction of Ag^+ ions to silver (Ag^0), facilitated by phytochemicals in the matoa leaf extract.²² The observed color change corresponds to the surface plasmon resonance (SPR) of the silver nanoparticles. This phenomenon is attributed to the collective oscillation of free electrons in the nanoparticles, which is induced by incident light.

The UV-Vis absorbances in Fig. 2b further confirm nanoparticle formation through the presence of characteristic SPR absorption bands. Distinct SPR peaks were observed at 434, 431, and 430 nm for samples synthesized at 360, 540, and 720 W, respectively. These results are consistent with the SPR peak characteristic for silver nanoparticles, which is typically centered around 400 nm.²³ In accordance with the Lambert-Beer law, the absorbance intensity is directly proportional to the analyte concentration. The higher irradiation power resulted in increased absorbance, indicating a greater nanoparticle yield.²⁴ It has been demonstrated that a blueshift in the SPR peak with increasing power is indicative of a reduction in nanoparticle size.²⁵ Furthermore, in the wavelength region below 330 nm, an increase in absorbance was observed, indicating the presence of residual phytochemicals from matoa leaf extract. A comparable absorption behavior has also been reported in AgNPs synthesized using water hyacinth leaf extract.⁷

FTIR analysis

Fourier-transform infrared (FTIR) spectroscopy was employed to identify the functional groups involved

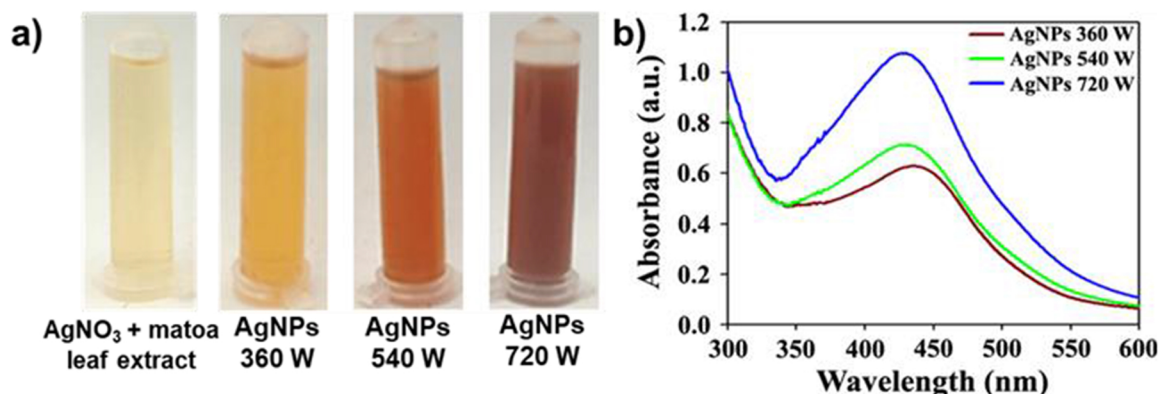


Fig. 2. (a) Bio-colloidal AgNPs samples and (b) UV-Vis absorption spectra of AgNPs synthesized at various microwave irradiation powers.

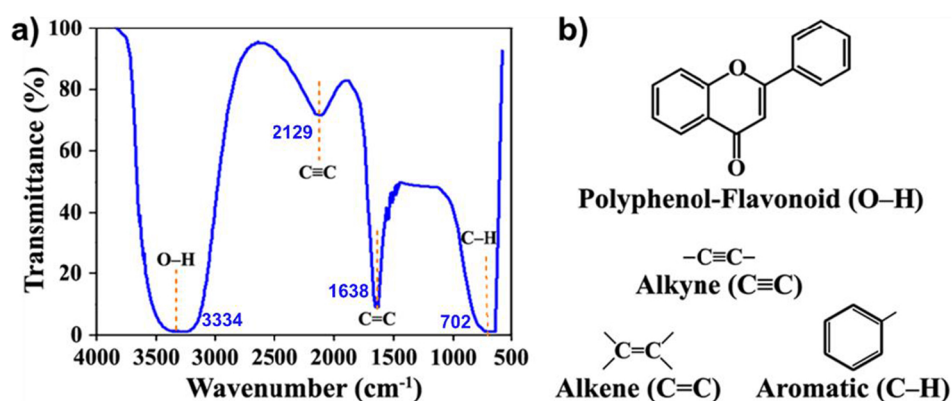


Fig. 3. (a) FTIR spectrum and (b) functional group structure present in AgNPs synthesized at irradiation power of 720 W.

in the formation of AgNPs, see Fig. 3a for the FTIR transmittance spectrum of the AgNP sample synthesized at 720 W, which was selected due to its highest SPR peak intensity. The spectrum thus reveals several characteristic absorption bands corresponding to functional groups from the matoa leaf extract. A broad band was observed at 3334 cm⁻¹, attributed to O-H stretching vibrations. This indicates the presence of polyphenolic compounds and hydroxyl groups (-OH) in flavonoids, see Fig. 3b for structure.²⁶ The hypothesis is that these substances act as reducing agents during the synthesis of nanoparticles. Furthermore, a peak at 2129 cm⁻¹ corresponds to the stretching vibration of the C≡C triple bond, indicating the presence of alkyne functional groups. A peak at around 1638 cm⁻¹ is assigned to C=C stretching alkenes, while the absorption at 702 cm⁻¹ is indicative of aromatic C-H bending vibration.²⁷ The presence of aromatic (C-H) and alcohol (O-H) functional groups serves to confirm the contribution of flavonoids and polyphenols from the matoa leaf extract in the reduction of Ag⁺ to Ag⁰. These phytochemicals not only act as reducing agents but also serve to stabilize the resulting AgNPs. Similar func-

tional group involvement has been reported in the biosynthesis of AgNPs using *Rosa indica* extract.²⁸

XRD analysis

As illustrated in Fig. 4a, the crystalline structure of was examined by X-ray diffraction analysis. The diffraction peaks observed at 2θ values of 38.59°, 44.65°, 64.64°, and 77.62° correspond to the (111), (200), (220), and (311) crystal planes, respectively. These peaks match well with the standard face-centered cubic (FCC) structure of silver (JCPDS No. 04-0783).²⁹ As illustrated in Fig. 4b, the crystal planes that contribute to this FCC structure are clearly evident.

The crystallite size of the AgNPs was estimated using the Debye-Scherrer equation, where the full width at half maximum (FWHM) values were obtained through Gaussian fitting. The calculation of lattice constants was performed utilizing the cubic crystal structure equation Table 1. presents the summary of FWHM, crystallite size, and lattice parameters of AgNPs. The calculated average crystallite

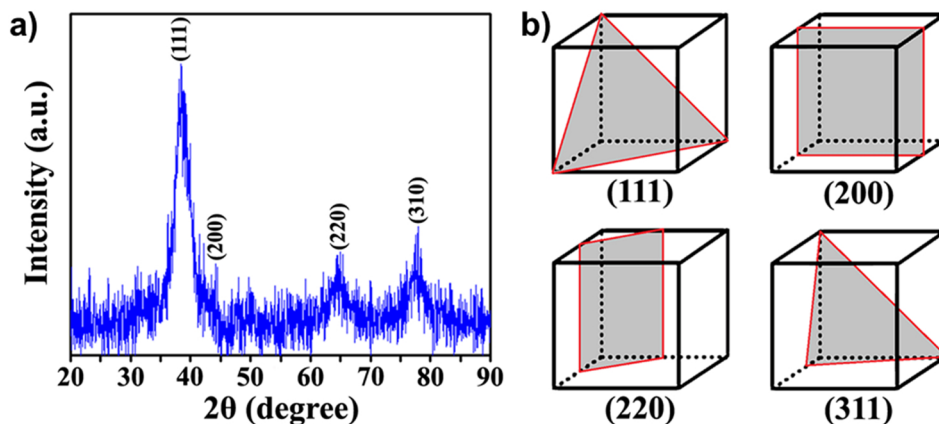


Fig. 4. (a) XRD pattern and (b) illustration of hkl planes forming a face-centered cubic structure of AgNPs synthesized at irradiation power of 720 W.

Table 1. XRD parameters of AgNPs.

hkl plane	2θ (°)	FWHM (°)	Crystallite size (nm)	Lattice constant (nm)
(111)	38.597	3.139	2.388	4.036
(200)	44.823	0.940	7.818	4.040
(220)	64.650	1.165	5.760	4.074
(311)	77.628	0.500	12.360	4.075

size and lattice constant of AgNPs were 7.082 nm and 4.056 nm, respectively, which are within the expected range for silver nanoparticles.³⁰ These results confirm the successful synthesis of crystalline AgNPs.

TEM morphology

Transmission Electron Microscopy (TEM) was employed to directly investigate the morphology and size distribution of silver nanoparticles (AgNPs), as depicted in Fig. 5. The micrographs show that most particles exhibit a quasi-spherical morphology, although a small fraction of anisotropic structures, including rod-like, triangular, prismatic, and polygonal forms, are also present. Such morphological diversity is commonly observed in previous studies that reported utilizing plant-based kiwi extract.¹⁶ The diameter sizes of AgNPs are 62.51, 59.63, and 58.84 nm at microwave powers of 360, 540, and 720 W, respectively. These results demonstrated that increasing the power of irradiation can reduce particle sizes with a narrower size distribution. It is also consistent with the results of UV-Vis spectroscopy, which revealed a blue shift in the SPR peak at higher irradiation power, indicating a decrease in particle size.

The size difference of AgNPs at higher irradiation power is attributable to enhanced nucleation rates, which are propelled by augmented kinetic energies.

Additionally, the presence of biomolecules in matoa leaf extract has been shown to play a stabilizing role by capping the surface of AgNPs. This, in turn, has been demonstrated to influence both particle growth and the resulting morphology.³¹

Sensing detection of mercury (II) ions

The sensing ability of the synthesized AgNPs to detect mercury(II) ions (Hg^{2+}) was investigated using a colorimetric approach. The ability of AgNPs to detect Hg^{2+} is indicated by the color change of the AgNPs when reacted with HgCl_2 , as demonstrated in Fig. 6a.

The color change in the AgNPs solution was found to be highly significant in relation to the increasing HgCl_2 concentration. It was observed that the synthesis of AgNPs at 360 W and 540 W resulted in a transition from a reddish-brown coloration to a pale yellow hue. In contrast, the synthesis at 720 W led to a transformation of AgNPs to a colorless state exhibiting a linear trend in the observed phenomenon. This finding suggests that the AgNPs, particularly those obtained at higher irradiation power, have the potential to be utilized for the visual detection of Hg^{2+} ions in water. The dramatic color change of the AgNP solution after the addition of Hg^{2+} is attributable to the formation of a silver-mercury complex, which is the consequence of the nano-sized silver particles, rendering them more reactive, and the strong affinity between silver and mercury.²⁷ Fig. 6b-d illustrates the UV-Vis absorption spectra of AgNPs following reaction with HgCl_2 at varying concentrations. The SPR peak of AgNPs was observed to decrease in a progressive manner and completely disappeared as the concentration of Hg^{2+} increased. The decline in SPR can be attributed primarily to the redox-driven

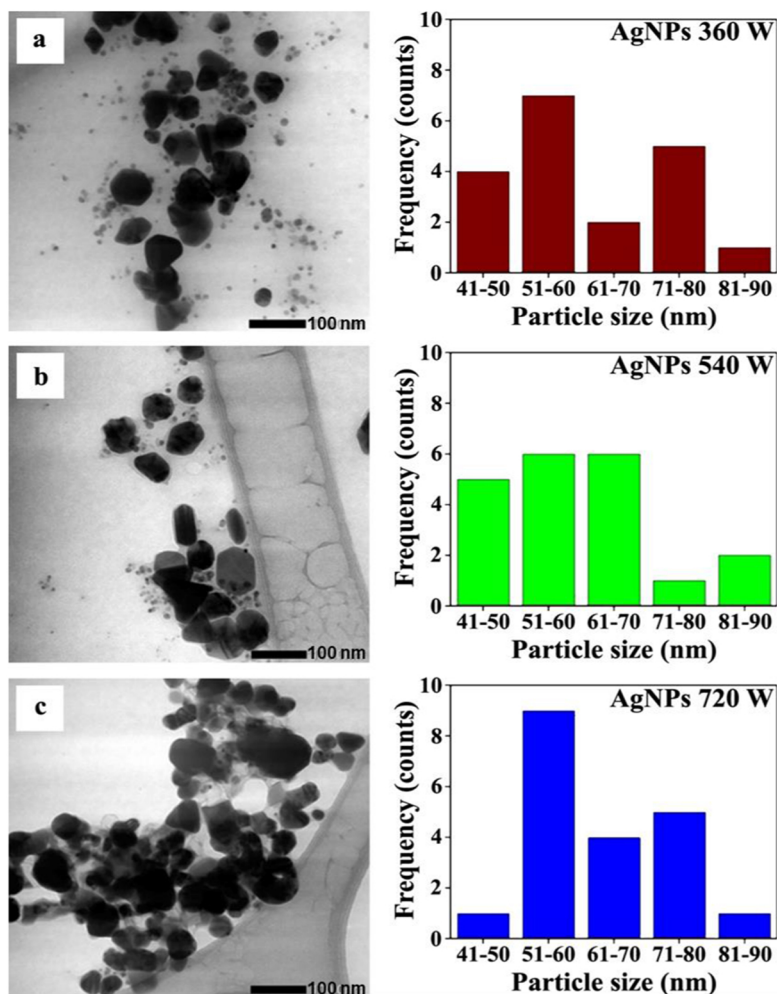


Fig. 5. TEM images accompanied bar histograms AgNPs with different microwave irradiation powers (a) 360 W, (b) 540 W, and (c) 720 W. Scale bar = 100 nm. The right panels show particle size distribution histograms derived from TEM measurements.

deposition of metallic mercury and nanoparticle aggregation. In the presence of elevated concentrations of Hg^{2+} ions, a redox reaction ensues between the metal nanoparticles (e.g., AgNPs or gold surfaces) and the Hg^{2+} ions. It has been demonstrated that Hg^{2+} is reduced to metallic Hg^0 , which then rapidly deposits onto the nanoparticle or sensor surface. The presence of a metallic Hg^0 film has been demonstrated to disrupt plasmonic resonance. AgNPs synthesized at 360 W demonstrated a substantial decrease and broadening of the SPR peak as the concentration of HgCl_2 increased, while those at 540 W and 720 W also experienced a sharp decrease in absorption. Increasing the concentration of HgCl_2 revealed a low absorption spectrum. This condition can be associated with an accelerated oxidation process within the AgNPs.³² In addition, the absorption peak of all AgNPs samples showed a blue-shift from 437 to 458 nm at the highest concentration of HgCl_2 . This

phenomenon is most likely related to the particle size reduction of AgNPs.^{33,34}

As shown in Fig. 7, a linear curve was observed between the SPR peak of AgNPs and Hg^{2+} ion concentration. The sensitivity of AgNPs to Hg^{2+} was determined from the slope of the absorbance curve at 433 nm. All samples exhibited two distinct linear ranges of sensitivity, specifically at Hg^{2+} ion concentrations of 0–40 ppm and 40–100 ppm. Within the lower Hg^{2+} ion concentration range (0–40 ppm), the slopes were -0.0051 , -0.0061 , and -0.0058 for AgNPs synthesized at 360, 540, and 720 W, respectively. At higher Hg^{2+} ion concentrations (40–100 ppm), the slopes decreased to -0.0005 , -0.0006 , and -0.0008 for AgNPs synthesized at 360, 540, and 720 W. This finding implies that as the slope becomes steeper, the Hg^{2+} detection of the AgNPs also increases. Notably, AgNPs synthesized at 720 W, which exhibited the highest SPR intensity and

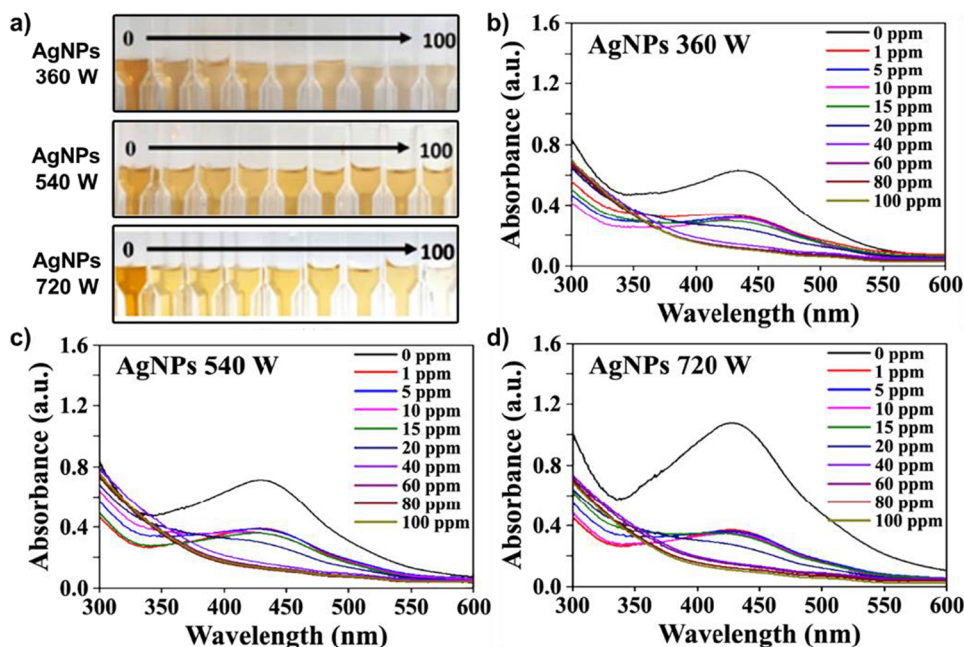


Fig. 6. (a) The appearance of bio-colloidal AgNPs discoloration; UV-Vis absorption spectra of bio-colloidal AgNPs treated with varying concentrations of HgCl_2 at microwave irradiation powers of (b) 360 W, (c) 540 W, and (d) 720 W.

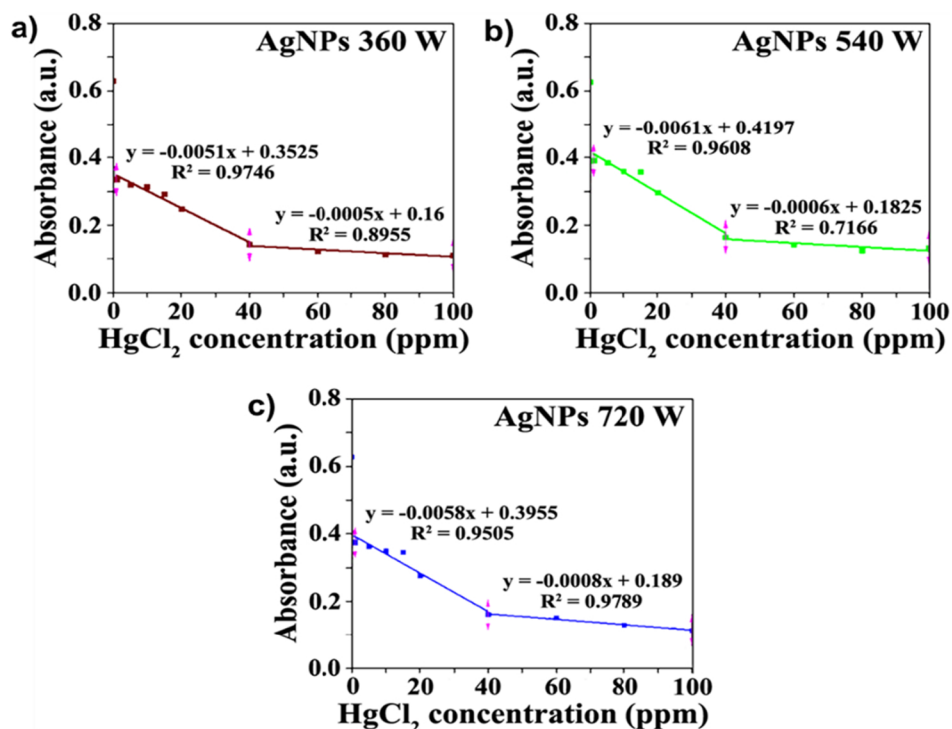


Fig. 7. Absorbance curve of AgNPs synthesized at microwave irradiation powers (a) 360 W, (b) 540 W, and (c) 720 W after the addition of various HgCl_2 concentrations.

smallest diameter size, showed complete disappearance of the SPR peak upon exposure to Hg^{2+} . This finding corroborates their high sensitivity towards lower Hg^{2+} concentrations. These observations re-

ported here are consistent with those reported in the earlier study, attributing the detection mechanism to the redox process. The utilization of AgNPs and Hg^{2+} in a colorimetric detection has been demonstrated to

elicit an oxidation-reduction reaction whereby AgNPs undergo oxidation to form Ag^+ and Hg^{2+} ions undergo reduction to form metallic Hg^0 atoms.³⁵ Whilst the detection limit in this study (1–100 ppm) exceeds the ppb sensitivity levels of certain contemporary state-of-the-art colorimetric sensors, the performance of the sensor in question is comparable to other plant-extract-mediated nanoparticle systems as reported in the extant literature.^{27,33} This sensitivity is adequate for detecting environmentally relevant Hg^{2+} concentrations, while offering additional advantages of simplicity, low cost, and green synthesis. It is evident from the findings of this study that bio-colloidal AgNPs synthesized in this work are capable of being an effective and reliable colorimetric detection of mercury (II) ion.

Conclusion

The utilization of matoa leaf extract in the synthesis of stable bio-colloidal AgNPs through microwave irradiation has been shown to yield favorable properties. The bio-colloidal AgNPs exhibited SPR peak broadening, effective reduction capability, spherical morphology, and crystalline structure. The sensitivity of bio-colloidal AgNPs to Hg^{2+} was clearly demonstrated by a distinct color change of the colloid from brownish yellow to colorless. The findings indicate that microwave-assisted green synthesis offers a straightforward, cost-effective, and eco-friendly approach to producing AgNPs with excellent potential as colorimetric sensors. The demonstrated sensitivity to the Hg^{2+} ion indicates that the bio-colloidal AgNPs are promising candidates for practical applications in environmental monitoring.

Acknowledgment

The authors would also like to express their gratitude to the Directorate of Research and Community Service, Ministry of Higher Education, Science and Technology of the Republic of Indonesia. And to LPPM (Lembaga Penelitian dan Pengabdian Masyarakat) at the University of Riau for their invaluable support in conducting this research.

Authors' declaration

- Conflicts of Interest: None.
- We hereby confirm that all the Figures and Tables in the manuscript are ours. Furthermore, any Figures and images that are not ours have been

included with the necessary permission for republication, which is attached to the manuscript.

- No animal studies are present in the manuscript.
- No human studies are present in the manuscript.
- Ethical Clearance: The project was approved by the local ethical committee at University of Riau.

Authors' contribution statement

A.S.R. designed the study and concept. A.S.R. and Y.R. analyzed data and interpretation. Y.R. and G.A.R. conducted the experiments and drafting the manuscript. A.S.R., Y.S and L.U performed revision and proofreading.

Data availability

The data that support the findings of this study are available on request from the corresponding author.

Funding statement

This present study is funded by the Directorate of Research and Community Service, Ministry of Higher Education, Science and Technology of the Republic of Indonesia, through the 2025 research grant.

References

1. Hasibuan DKA, Riani E, Anwar S. Mercury (Hg) contamination in river water, well water, sediment and fish in Kuantan River, Riau. *JPSL*. 10(4):679–687. <http://dx.doi.org/10.29244/jpsl.10.4.679--687>.
2. Wang L, Hou D, Cao y, Ok YS, Tack FMG, Rinklebe J, *et al*. Remediation of mercury contaminated soil, water, and air: A review of emerging materials and innovative technologies. *Environ Int*. 2020;134:105281. <https://doi.org/10.1016/j.envint.2019.105281>.
3. Fu LM, Hsu JH, Shih MK, Hsieh CW, Ju WJ, Chen YW, *et al*. Process optimization of silver nanoparticle synthesis and its application in mercury detection. *Micromachines*. 2021; 12(9):1–16. <https://doi.org/10.3390/mi12091123>.
4. Meenakshi S, Devi S, Pandian K, Chitra K, Tharmaraj P. Aniline-mediated synthesis of carboxymethyl cellulose protected silver nanoparticles modified electrode for the differential pulse anodic stripping voltammetry detection of mercury at trace level. *Ionics (Kiel)*. 2019;25(7):3431–3441. <https://doi.org/10.1007/s11581-019-02858-0>.
5. Bhatt KD, Vyas DJ, Makwana BA, Darjee SM, Jain VK, Shah H. Turn-on fluorescence probe for selective detection of Hg(II) by calixpyrrole hydrazide reduced silver nanoparticle: Application to real water sample. *Chinese Chem Lett*. 2016; 27(5): 731–737. <https://doi.org/10.1016/j.ccllet.2016.01.012>.
6. Tsegay MG, Gebretinsae HG, Sackey J, Maaza M, Nuru ZY. Green synthesis of khat mediated silver nanoparticles for efficient detection of mercury ions. *Mater Today Proc*.

- 2019; 36(2):368–373. <https://doi.org/10.1016/j.matpr.2020.04.217>.
7. Oluwafemi OS, Anyik JL, Zikalala NE, Sakho EHM. Biosynthesis of silver nanoparticles from water hyacinth plant leaves extract for colourimetric sensing of heavy metals. *Nano-Structures and Nano-Objects*. 2019;20:100387. <https://doi.org/10.1016/j.nanoso.2019.100387>.
 8. Firdhouse MJ, Lalitha P. Biosynthesis of silver nanoparticles and its applications. *J Nanotechnol*. 2015;2015(1):829526. <https://doi.org/10.1155/2015/829526>.
 9. Henríquez LC, Aguilar KA, Alvarez JU, Fernández LV, Vásquez GMO, Baudrit JRV. Green synthesis of gold and silver nanoparticles from plant extracts and their possible applications as antimicrobial agents in the agricultural area. *Nanomaterials*. 2020;10(9):1–24. <https://doi.org/10.3390/nano10091763>.
 10. Yılmaz DD, Demirezen DA, Mihçioğur H. Colorimetric detection of mercury ion using chlorophyll functionalized green silver nanoparticles in aqueous medium. *Surf Interfaces*. 2020;22:100840. <https://doi.org/10.1016/j.surfin.2020.100840>.
 11. Alnuaimi MT, Aljanabi ZZ, Mahmood SI, Ramzy UF. Production of biosynthesized silver nanoparticles using metarhizium anisopliae fungus for the treatment of petroleum pollutants in water. *Baghdad Sci J*. 2024;21(6):1935–1952. <https://dx.doi.org/10.21123/bsj.2023.8577>.
 12. Bashir F, Sharif S, Manzoor F, Naz S, Rashid F. Protective effects of *Moringa oleifera* leaf extract against silver nanoparticles and arsenic induced hepatotoxicity in rats. *Pak. Vet. J*. 2024;44:377–383. <http://dx.doi.org/10.29261/pakvetj/2024.154>.
 13. Ertürk AS. Biosynthesis of silver nanoparticles using epilobium parviflorum green tea extract: analytical applications to colorimetric detection of Hg^{2+} ions and reduction of hazardous organic dyes. *J Clust Sci*. 2019;30(5):1363–1373. <https://doi.org/10.1007/s10876-019-01634-4>.
 14. Siddiqi KS, Husen A, Rao RAK. A review on biosynthesis of silver nanoparticles and their biocidal properties. *J Nanobiotechnology*. 2018;16(1):1–28. <https://doi.org/10.1186/s12951-018-0334-5>.
 15. Samari F, Salehipoor H, Eftekhar E, Yousefinejad S. Low-temperature biosynthesis of silver nanoparticles using mango leaf extract: catalytic effect, antioxidant properties, anticancer activity and application for colorimetric sensing. *New J Chem*. 2018;42(19):15905–15916. <https://doi.org/10.1039/C8NJ03156H>.
 16. Devadiga A, Shetty KV, Saidutta MB. Highly stable silver nanoparticles synthesized using Terminalia catappa leaves as antibacterial agent and colorimetric mercury sensor. *Mater Lett*. 2017;207:66–71. <https://doi.org/10.1016/j.matlet.2017.07.024>.
 17. Gomathi E, Jayapriya M, Arulmozhi M. Environmental benign synthesis of tin oxide (SnO_2) nanoparticles using *Actinidia deliciosa* (Kiwi) peel extract with enhanced catalytic properties. *Inorg Chem Commun*. 2021;130:108670. <https://doi.org/10.1016/j.inoche.2021.108670>.
 18. Carmona ER, Benito N, Plaza T, Sánchez GR. Green synthesis of silver nanoparticles by using leaf extracts from the endemic *Buddleja globosa* hope. *Green Chem Lett Rev*. 2017;10(4):250–256. <https://doi.org/10.1080/17518253.2017.1360400>.
 19. Uddin I, Ahmad K, Khan AA, Kazmi MA. Synthesis of silver nanoparticles using *Matricaria recutita* (Babunah) plant extract and its study as mercury ions sensor. *Sens Bio-Sensing Res*. 2017;16:62–67. <https://doi.org/10.1016/j.sbsr.2017.11.005>.
 20. Handayani W, Ningrum AS, Imawan C. The role of pH in synthesis silver nanoparticles using *Pometia pinnata* (Matoa) leaves extract as bioreductor. *J Phys.:Conf Ser*. 2020;1428:012021. <https://doi.org/10.1088/1742-6596/1428/1/012021>.
 21. Altarjami LR. Anticancer and antioxidant activities of polyphenolic pomegranate peel extracts obtained by a novel hybrid ultrasound-microwave method: in vitro and in vivo studies in albino mice with HeLa, Colon, and HepG2 Cancerous Cell Lines. *Pak Vet J*. 2025;45(2):723–734. <http://dx.doi.org/10.29261/pakvetj/2025.154>.
 22. Joseph S, Mathew B. Microwave assisted biosynthesis of silver nanoparticles using the rhizome extract of alpinia galanga and evaluation of their catalytic and antimicrobial activities. *J Nanoparticles*. 2014;2014(1):967802. <https://doi.org/10.1155/2014/967802>.
 23. Jain N, Jain P, Rajput D, Patil UK. Green synthesized plant-based silver nanoparticles: therapeutic prospective for anticancer and antiviral activity. *Micro Nano Syst Lett*. 2021;9(1):1–24. <https://doi.org/10.1186/s40486-021-00131-6>.
 24. Ningrum AS, Pridyantari AP, Handayani W, Secario K, Djuhana D, Imawan C. Green synthesis of silver nanoparticles using leaf and stem bark extract of *Pometia pinnata* J.R. Forst & G. Forst. *IOP Conf Ser: Earth Environ Sci*. 2020;481: 012018. <https://doi.org/10.1088/1755--1315/481/1/012018>.
 25. Barani H, Mahltig B. Microwave-assisted synthesis of silver nanoparticles: effect of reaction temperature and precursor concentration on fluorescent property. *J Clust Sci*. 2022;33(1):101–111. <https://doi.org/10.1007/s10876-020-01945-x>.
 26. Raza S, Yan W, Stenger N, Wubs M, Mortensen NA. Blueshift of the surface plasmon resonance in silver nanoparticles: substrate effects. *Opt Express*. 2013;21(22):27344. <https://doi.org/10.1364/oe.21.027344>.
 27. Rini AS, Adzani H, Husain TSL, Deraf MP, Rati Y, Hamzah Y. Structural and morphological studies of silver nanoparticles prepared using citrullus lanatus rind extract. *AIP Conf Proc*. 2021;2320:1–6. <https://doi.org/10.1063/5.0037960>.
 28. Aminu A, Oladepo SA. Fast orange peel-mediated synthesis of silver nanoparticles and use as visual colorimetric sensor in the selective detection of mercury (II) ions. *Arab J Sci Eng*. 2021;46:5477–5487. <https://doi.org/10.1007/s13369-020-05030-3>.
 29. Raj A, Lawrence R, Lawrence K, Silas N, Jaless M, Srivastava R. Green synthesis and characterization of silver nanoparticles from leaf extracts of *rosa indica* and its antibacterial activity against human pathogen bacteria. *Orient J Chem*. 2018;34(1):326–335. <https://doi.org/10.13005/ojc/340135>.
 30. Seku K, Gangapuram BR, Pejjai B, Kadimpati KK, Golla N. Microwave-assisted synthesis of silver nanoparticles and their application in catalytic, antibacterial and antioxidant activities. *J Nanostructure Chem*. 2018;8(2):179–188. <https://doi.org/10.1007/s40097-018-0264-7>.
 31. Saleh TA, Majeed S, Nayak A, Bhushan B. Principles and advantages of microwave-assisted methods for the synthesis of nanomaterials for water purification. *Adv Nanomater Water Eng Treat Hydraul*. 2017;40:–57. <https://doi.org/10.4018/978-1-5225-2136-5.ch003>.
 32. Wang A, Yang F, Yang X. Colorimetric detection of mercury(II) ion using unmodified silver nanoparticles and mercury-specific oligonucleotides. *ACS Appl Mater Interfaces*. 2010;2(2):339–342. <https://doi.org/10.1021/am9007243>.
 33. Firdaus ML, Fitriani I, Wyanatuti S, Hartati YW, Khaydarov R, Mcelister JA, et. al. Colorimetric detection of mercury

- (II) ion in aqueous solution using silver nanoparticles. *J Jpn Soc Anal Chem.* 2017;33(201):831–837. <https://doi.org/10.2116/analsci.33.831>.
34. Rini AS, Fitriasia A, Rati Y, Umar L, Soerbakti Y. Bio-colloidal silver nanoparticles prepared via green synthesis using *sandoricum koetjape* peel extract for selective colorimetry-based mercury ions detection. *KIJOMS.* 2023;9(2):280–288. <https://doi.org/10.33640/2405-609X.3299>.
35. Kumar V, Singh DK, Mohan S, Bano D, Gundampati RK, Hasan SH. Green synthesis of silver nanoparticle for the selective and sensitive colorimetric detection of mercury (II) ion. *J Photochem Photobiol B.* 2017;168:67–77. <https://doi.org/10.1016/j.jphotobiol.2017.01.022>.

الكشف عن أيونات الزئبق الثنائي (II) المعتمد على القياس اللوني باستخدام جسيمات الفضة النانوية الغروية الحيوية المُحضَّرة عبر التخليق الأخضر المدعوم بالميكروويف باستخدام مستخلص أوراق الماتوا

أري سوليستيو ريني¹، يولاندا راتي²، غيلار عدنان رمضان¹، يان سورباكتي¹، لازوآردي عمر¹

¹ قسم الفيزياء، كلية الرياضيات والعلوم الطبيعية، جامعة رياو، بيكانبارو 28293، إندونيسيا.

² قسم الفيزياء، كلية العلوم، معهد تكنولوجيا سومطرة، لامبونج سيلاتان 35365، إندونيسيا.

الملخص

في هذا العمل، تم تحضير جسيمات الفضة النانوية الغروية الحيوية (AgNPs) باستخدام مستخلص أوراق الماتوا (*Pometia pinnata*) كعامل مختزل ومثبّت تحت تأثير إشعاع الميكروويف لتعزيز التكوين السريع لجسيمات الفضة النانوية. وقد تمّت دراسة تأثير قدرات إشعاع الميكروويف (360، 540، و720 واط) بصورة منهجية على الخصائص البصرية والتركيبية والمورفولوجية لجسيمات الفضة النانوية المُحضَّرة. تم تأكيد تكوّن جسيمات الفضة النانوية من خلال ظهور محاليل غروية ذات لون أصفر مائل إلى البني مع نطاقات رنين بلازمون السطح (SPR) متمركزة حول 430 نانومتر، كما تم الكشف عنها بواسطة مطيافية الأشعة فوق البنفسجية-المرئية (UV-Vis) وكشف تحليل FTIR عن وجود مجاميع وظيفية من نوع C-H و O-H تعود إلى المركبات متعددة الفينولات والفلافونويدات، والتي ساهمت في اختزال أيونات Ag⁺ وأظهر نمط حيود الأشعة السينية (XRD) بنية بلورية مكعبة متمركزة الوجوه (FCC) لجسيمات الفضة النانوية، في حين أظهرت صور المجهر الإلكتروني النافذ (TEM) شكلاً شبه كروي غالباً بمتوسط قطر يتراوح بين 58-62 نانومتر. تم تقييم أداء التحسس اللوني ضمن مدى تركيز لأيونات الزئبق الثنائي (Hg²⁺) يتراوح بين 1-100 جزء في المليون (ppm) وعند تعريض الجسيمات لأيونات Hg²⁺، أظهرت المحاليل الغروية انخفاضاً تدريجياً في شدة نطاق SPR مصحوباً بتغير لوني ملحوظ في المجال 350-550 نانومتر. وأظهرت الجسيمات النانوية المُحضَّرة عند قدرة 720 واط أعلى حساسية، حيث لوحظ تغير لوني واضح ضمن مدى تركيز 40-100 جزء في المليون من Hg²⁺، مع أكبر ميل مقداره 8×10^{-4} . تُبرز هذه النتائج الإمكانية الواعدة لاستخدام جسيمات الفضة النانوية المستخلصة من *Pometia pinnata* والمُحضَّرة بمساعدة الميكروويف كنهج أخضر وصدّيق للبيئة للكشف اللوني عن أيونات الزئبق.

الكلمات المفتاحية: غروي حيوي، أيونات الزئبق (II)، التخليق بمساعدة الميكروويف، أوراق *Pometia pinnata*، جسيمات الفضة النانوية.